Quantum Electronics **44** (12) 1129–1135 (2014)

OPTICAL FIBRES

PACS numbers: 42.81.Cn; 42.81.Dp; 32.80.–t
DOI: 10.1070/QE2014v044n12ABEH015622

Charge-transfer state excitation as the main mechanism of the photodarkening process in ytterbium-doped aluminosilicate fibres

K.K. Bobkov, A.A. Rybaltovsky, V.V. Vel'miskin, M.E. Likhachev, M.M. Bubnov, E.M. Dianov, A.A. Umnikov, A.N. Gur'yanov, N.N. Vechkanov, I.A. Shestakova

Abstract. **We have studied photodarkening in ytterbium-doped fibre preforms with an aluminosilicate glass core. Analysis of their absorption and luminescence spectra indicates the formation of stable Yb^{2+} ions in the glass network under IR laser pumping at a wavelength λ = 915 nm and under UV irradiation with an excimer laser (λ = 193 nm). We have performed comparative studies of the luminescence spectra of the preforms and crystals under excitation at a wavelength of 193 nm. The mechanism behind the formation of Yb^{2+} ions and aluminium–oxygen hole centres (Al-OHCs), common to ytterbium-doped YAG crystals and aluminosilicate glass, has been identified: photoinduced Yb^{3+} charge-transfer state excitation.**

Keywords: *photodarkening, divalent ytterbium ions, ytterbium-doped active fibres, fibre laser, charge transfer, oxygen hole centres.*

1. Introduction

Optical fibres with an ytterbium-doped silica core are widely used in producing high-power fibre lasers. Technologically, it is convenient to use silica glass with small alumina additions (of the order of several mole percent), because it is such a host that enables high ytterbium ion concentrations to be reached. The output power of lasers based on such fibres was, however, found to gradually decrease during long-term operation. As first shown in 2005 [1], the degradation of ytterbium-doped fibre lasers is caused by photoinduced optical losses in the fibre, which increase sharply in the short-wavelength range. Somewhat later, in 2007, Shubin et al. [2] and Manek–Hönninger et al. [3] found independently that the photoinduced loss curve had a pronounced maximum near a wavelength of 500 nm. The band centred around 500 nm was shown to make a decisive contribution to the photoinduced loss in the operating spectral range of ytterbium-doped fibre lasers and amplifiers (900–1100 nm) and to originate from the absorption by aluminium–oxygen hole centres (Al-OHCs), which are usually produced in the aluminosilicate glass network by UV or gamma radiation [4, 5]. It should be emphasised in this context that photoinduced Al-OHC generation in the photodarkening process has been demonstrated not only by optical methods but also by detecting EPR lines corresponding to these centres [4]. At the same time, the mechanism of IR-pumping-induced Al-OHC generation in ytterbium-doped fibres is still the subject of controversy. The purpose of this work is to validate one proposed model based on photoinduced charge transfer.

K.K. Bobkov, A.A. Rybaltovsky, V.V. Vel'miskin, M.E. Likhachev, M.M. Bubnov, E.M. Dianov Fiber Optics Research Center, Russian Academy of Sciences, ul. Vavilova 38, 119333 Moscow, Russia; e-mail: wittkoss@gmail.com, rybaltovsky@yandex.ru, likhachev@fo.gpi.ru, bubnov@fo.gpi.ru, dianov@fo.gpi.ru;
A.A. Umnikov, A.N. Gur'yanov, N.N. Vechkanov G.G. Devyatykh Institute of Chemistry of High-Purity Substances, Russian Academy of Sciences, ul. Tropinina 49, 603950 Nizhnii Novgorod, Russia; e-mail: umnikov@ihps.nnov.ru, guryanov@ihps.nnov.ru, tvs@ihps.nnov.ru;
I.A. Shestakova OJSC M.F. Stel'makh Polyus Research Institute, ul. Vvedenskogo 3/1, 117342 Moscow, Russia

Received 11 July 2014; revision received 23 September 2014
Kvantovaya Elektronika **44** (12) 1129–1135 (2014)
Translated by O.M. Tsarev

2. Mechanisms of Al-OHC generation

It is commonly believed that the main mechanism of Al-OHC generation in silica glass is the UV or gamma radiation-induced breaking or severe distortion (elongation) of Al–O–Si bridge bonds [6, 7]. This means that an energy of several electronvolts is necessary, which is several times the photon energy of IR pumping and Yb^{3+} luminescence (~1.3 eV). In view of this, it was assumed that, in the glass network, such energy could be provided by interaction in a cluster of (three to seven) closely spaced excited Yb^{3+} ions [2, 8, 9]. This assumption rests on analysis of the measured photoinduced loss as a function of fibre core composition and IR irradiation conditions, which demonstrates that the photoinduced optical loss saturation is a power law function of ytterbium ion concentration in the fibre and population inversion [1, 8, 9].

The structure of ion clusters in glass is still the subject of detailed discussion. In a model that is thought to be the most likely, two nearest neighbour ytterbium ions are only separated by one oxygen (Yb–O–Yb bonds). This configuration is an approximate analogue of a structural element of ytterbium oxide (Yb_2O_3). The use of echo-detected EPR for probing the Yb^{3+} f-electron shell and a method that takes into account the hyperfine interaction between the electron and nuclear spin magnetic moments made it possible to detect an electron spin echo signal from ionic clusters at zero magnetic field in $Yb_2O_3:GeO_2$ [10] and $Yb_2O_3:Al_2O_3:SiO_2$ [11] glasses, which lends support to the above hypothesis, because the EPR spectrum of 'pure' Yb_2O_3 also contains such a signal.

To date, several modes have been proposed to gain insight into the mechanism of IR-radiation-induced Al-OHC generation in ytterbium-doped fibre cores. These models can be divided into two groups: models that consider the excitation of oxygen-deficient centres and those that deal with charge-transfer state excitation.

3. Excitation of oxygen-deficient centres

In a number of studies [12–14], Al-OHC generation in a glass network was interpreted in terms of the primary ionisation of oxygen-deficient centres (ODCs). As shown earlier [15], ionised ODCs in silica glass are sources of self-trapped holes, which may subsequently be localised (trapped) at one of the nearest neighbour bridging oxygens to form an OHC [16]. Since the ODCs show the strongest absorption at wavelengths under 250 nm, excitation of these centres requires simultaneous energy transfer from four or more Yb^{3+} ions, i.e. at least 5 eV. Some reports, however, proposed taking into account not only the direct excitation of an ODC by a UV photon of appropriate energy (above 5 eV) but also 'cascade' excitation in which the role of 'intermediate' energy levels is played by levels of other defects: nonbridging oxygen hole centres (NBOHCs) [17] or other rare-earth ions, e.g. thulium [18]. The energy of two or three excited Yb^{3+} ions is then sufficient for photoinduced Al-OHC generation.

This model has some drawbacks. For example, known attempts to experimentally detect UV photons resulting from the summation of the energies of four (250 nm) or, more likely, three (330 nm) Yb^{3+} ions were unsuccessful [18, 19]. Moreover, ODC excitation in silica glass is known to result in characteristic luminescence bands, centred at 4.4 and 2.7 eV in the case of silicon-related ODCs [20] and at 4.3 and 3.1 eV in the case of GeODCs [21]. Under IR irradiation, however, these bands were only observed in glass additionally doped with germanium [19], even though there are many reports on Al-OHC generation in germanium-free fibres. It is also worth noting that, during drawing, fibres are exposed to UV radiation with a photon energy sufficient for photoinduced Al-OHC generation [17], but such centres are known not to form in this process.

Thus, we believe that, even though ODC excitation makes some contribution to the Al-OHC formation mechanism, this contribution is not crucial.

4. Charge-transfer state excitation

According to a number of researchers [22, 23], IR-pumping-induced Al-OHC generation in active fibres is due to photo-induced charge transfer. It is worth noting that this effect has been studied for a number of rare-earth ions (Sm, Tb and Er) in aluminosilicate fibres [24, 25], whereas Yb^{3+} charge transfer was first detected in ytterbium-doped aluminate crystals [26, 27]. According to the model in question, Yb^{3+} ions in crystals and glass are surrounded by oxygens and, as a consequence, have an additional energy level corresponding to a so-called charge transfer state (CTS). CTS excitation may initiate an electron transition from nearest neighbour oxygens to the Yb^{3+} ion, leading to the formation of a defect pair: Yb^{2+} ion + OHC. Given that ytterbium ions in aluminosilicate glass are surrounded predominantly by AlO_4 tetrahedra [28], Al-OHCs are most likely to be involved.

In our opinion, however, there is still no conclusive evidence that Yb^{3+} ions in aluminosilicate glass have CTS levels or that there is a photoinduced $Yb^{3+} \rightarrow Yb^{2+}$ transition due to excitation of the ions. In particular, the absorption band centred at 230–240 nm in the spectrum of ytterbium-doped aluminosilicate glass is assigned to the transition of Yb^{3+} to a CTS by some researchers [5, 22, 23] and to absorption in ODCs by others [12–14]. The formation of Yb^{2+} ions in the aluminosilicate glass network as a result of photoinduced CTS excitation also requires additional evidence, because the presence of Yb^{2+} ions as a result of UV or IR irradiation has so far been inferred only from irradiation-induced changes in the luminescence spectrum of the material [23, 29, 30]. However, the peak emission wavelength in the luminescence band of Yb^{2+} in aluminosilicate glass has variously been reported as 700 [29], 390 [30] and 530 nm [23]. Finally, it is worth pointing out that visible luminescence may also be due to ODCs or NBOHCs [13, 17].

The purpose of this work was to provide experimental evidence of photoinduced charge transfer in ytterbium-doped aluminosilicate fibres and demonstrate that, as a result of charge transfer state excitation, some of the Yb^{3+} ions are reduced to Yb^{2+}. To this end, we compared the luminescence and absorption spectra of Yb:YAG crystals, in which charge transfer has been studied in detail, and those of Al_2O_3:Yb_2O_3:SiO_2 glass.

5. Experimental

We studied transverse sections of fibre preforms with Al_2O_3:Yb_2O_3:SiO_2 glass cores and those of an ytterbium-doped yttrium aluminium garnet (Yb:$Y_3Al_5O_{12}$, or Yb:YAG) crystal. Thin transverse sections of the preforms were used instead of pieces of fibres since the absorption in such fibres cannot be measured at wavelengths under 400 nm because of the large absorption loss. Yb:YAG was chosen for comparative studies of absorption and luminescence spectra because there is a large body of spectroscopic data for Yb:YAG crystals and because the nearest neighbour environment of the ytterbium ion in this material is similar to that in aluminosilicate glass [31–33]. The chemical composition of the preforms and crystal was determined with an accuracy of 0.02 wt% by X-ray microanalysis on a JEOL JSM-5910LV. The chemical compositions of the samples are listed in Table 1.

Initial and photoinduced absorption spectra in the UV and visible spectral regions (160–800 nm) and luminescence

Table 1. Main characteristics of the preforms and crystal.

Sample	Fabrication process	Chemical composition	wt% Yb	wt% Al	Oxidation state of Yb
A	Czochralski pulling	Yb:$Y_3Al_5O_{12}$	0.21	21.2	+3
B	MCVD	Al_2O_3:Yb_2O_3:SiO_2	0.2	1.8	+3
C	MCVD	Al_2O_3:SiO_2	0	1.7	–
D	Powder-in-tube	Al_2O_3:Yb_2O_3:SiO_2	0.1	1.5	+2, +3

spectra were taken using transverse sections of the preforms and sections of the crystal 0.2 and 1 mm in thickness.

Prior to UV irradiation, some of the preforms were exposed to a hydrogen atmosphere for six days at 110 °C and 115 atm. In this way, sections of the preforms were loaded with molecular hydrogen in order to examine its effect on the photoinduced formation of colour centres in the glass network.

We used two radiation sources: an Oclaro BMU25A-915-01-R laser diode module (915 nm) and a CL-5000 ArF excimer laser (193 nm). In both cases, the laser beam was focused onto the preform core.

The absorption spectra of the preforms were measured on a McPherson VUVAS 1000 vacuum spectrophotometer at wavelengths shorter than 190 nm (vacuum UV) and on a PerkinElmer Lambda 900 spectrophotometer in the range 190–850 nm. The luminescence spectra were obtained with an Ocean Optics Maya 2000 Pro minispectrometer.

All irradiations, as well as the luminescence and photoinduced absorption measurements, were performed at room temperature.

6. Results

Figure 1 shows the initial UV absorption spectra of the Yb:YAG crystal (A) and $Al_2O_3:Yb_2O_3:SiO_2$ (B) and $Al_2O_3:SiO_2$ (C) preforms. The shape of the spectrum of sample B was analysed by fitting with Gaussians using a standard procedure, which allowed us to identify two bands, peaking at 5.1 and 6.5 eV. Different origins of these bands were proposed in the literature. In particular, the absorption in the range 5–6 eV was assigned to different types of ODCs (Si-, Ge- and Yb-ODCs) [12, 13] or to Yb^{3+} transitions to a CTS in the glass network [22, 23]. The latter model stems from the known energy level diagram of the Yb^{3+} ion in doped crystals, where the existence of a CTS was confirmed by both experimental data [26, 27] and quantum-chemical calculations [34]. Note that the spectrum of sample C ($Al_2O_3:SiO_2$ preform) shows no absorption near 5 eV (Fig. 1), which demonstrates that the absorption in question is due to the presence of ytterbium ions in the glass network, rather than to ODCs with an unknown structure.

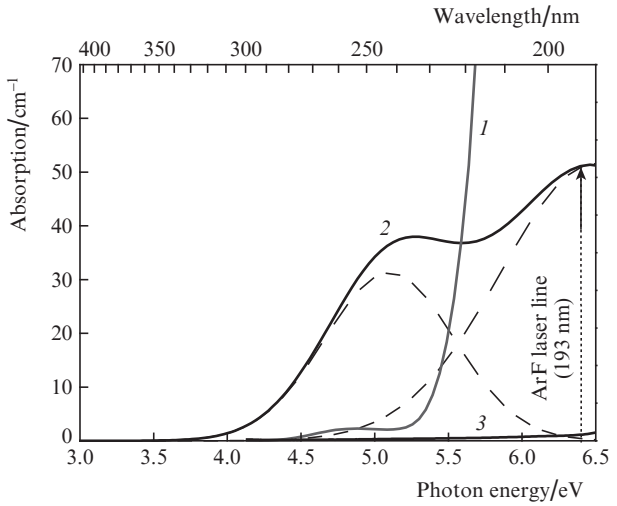

Figure 1. Initial UV absorption spectra of samples (*1*) A, (*2*) B and (*3*) C.

To gain insight into the structure of the colour centres, we compared the luminescence spectra of crystal A and preform B (Fig. 2) measured under ArF excimer laser irradiation (wavelength, 193 nm; photon energy, 6.4 eV). The spectrum of sample A showed two luminescence bands, peaking at 2.6 and 3.6 eV, and the short-wavelength edge of Yb^{3+} IR luminescence. Based on previously reported luminescence spectra of Yb:YAG [26, 27], the bands at 2.6 and 3.6 eV were assigned to the CTS → $^2F_{5/2}$ and CTS → $^2F_{7/2}$ radiative transitions, respectively (Fig. 3). By comparing the position of the charge transfer luminescence (CTL) bands with the energy level diagram of the Yb^{3+} ion in Fig. 3, it is easy to show that, independent of the host, the energy separation between the two CTL bands is roughly equal to the energy of the $^2F_{5/2} \rightarrow {}^2F_{7/2}$ transition: ~1 eV. Assuming that the local Yb^{3+} environment in the glass is similar to that in the Yb:YAG crystal, we expected to find CTL bands in preform B in roughly the same spectral region. As seen in Fig. 2, the luminescence spectrum of sample B contains bands peaking at 2.3 and 3.5 eV and the Yb^{3+} IR luminescence edge. Assigning the 2.3- and 3.5-eV bands to CTL, we confirmed that the photoinduced CTS excitation process in the glass is similar to that in the crystal.

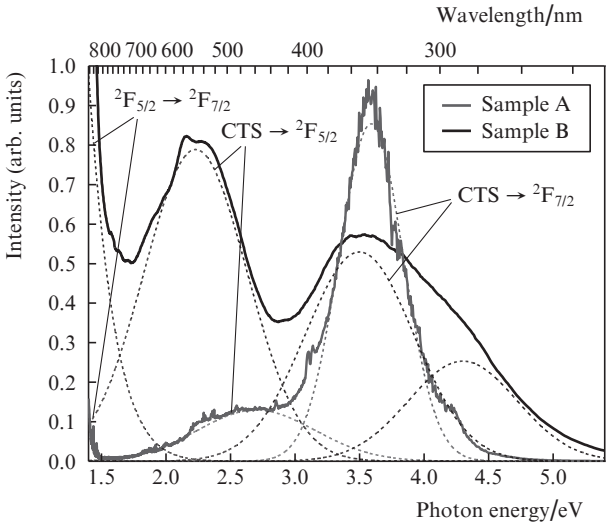

Figure 2. Normalised luminescence spectra of samples A and B under ArF laser excitation at a wavelength of 193 nm (6.4 eV).

According to Guerassimova et al. [27] and Krasikov et al. [34], one possible relaxation path of Yb^{3+} excited to a CTS in aluminate crystals is electron capture from one of the nearest neighbour oxygens, which leads to the reduction of the Yb^{3+} ion to a divalent state. Simultaneously, an OHC should appear near the Yb^{2+} ion formed. Given that ytterbium ions in $Al_2O_3:Yb_2O_3:SiO_2$ glass are surrounded predominantly by AlO_4 tetrahedra, an Al-OHC is most likely to form. Thus, the photochemical reaction involving Yb^{3+} ions and nearest neighbour atoms can be represented by the scheme

$$Yb^{3+}-O-Al \overset{h\nu}{\longleftrightarrow} Yb^{2+} + {}^{\circ}O-Al \qquad (1)$$

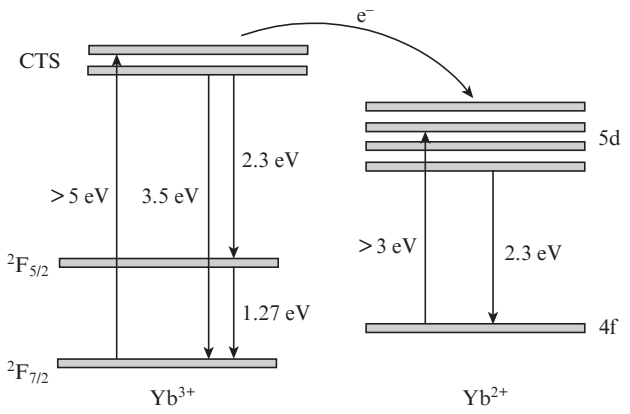

Figure 3. Model of Yb^{3+} excitation to a CTS and a possible transition of Yb^{3+} to Yb^{2+}.

(the superscript ° denotes a hole localised at an oxygen atom, which is identical to an Al-OHC).

It is worth noting, however, that, under UV irradiation, the $Yb^{3+} \rightarrow Yb^{2+}$ transition and photoinduced Al-OHC generation near Yb^{2+} result from direct CTS excitation by a high-energy photon, whereas under IR irradiation these processes are due to so-called cooperative excitation by the sum energy of a cluster of several closely spaced Yb^{3+} ions. A model for such cooperative CTS excitation, based on energy transfer between neighbouring Yb^{3+} ion pairs (ytterbium dimers), was proposed previously for Yb:YAG crystals [35]. In this model, emission from a pair of simultaneously excited Yb^{3+} ions is the well-known ~2.6-eV cooperative luminescence in crystals and glasses. The absorption of a photon of this luminescence by a neighbouring pair of excited ions, resulting in CTS excitation ($2.6 \times 2 = 5.2$ eV), is far more likely than the process proposed by Jetschke et al. [8]: generation of UV photons of energy $E \geqslant 5$ eV as a result of multiple pump photon or ~1.3-eV Yb^{3+} luminescence absorption.

The next step of our work was to provide evidence of partial $Yb^{3+} \rightarrow Yb^{2+}$ ion conversion in the case of Yb^{3+} CTS excitation in $Al_2O_3:Yb_2O_3:SiO_2$ glass. Yb^{2+} ions in aluminate crystals are known to have several absorption bands in the UV spectral region, at 410, 345 and 300 nm (3, 3.6 and 4.1 eV), corresponding to transitions from the 4f ground state to 5d excited states [36]. Similar absorption bands were observed in the spectrum of aluminosilicate glass prepared in a reducing atmosphere [22, 37]. According to Henke et al. [36], the radiative relaxation of excited Yb^{2+} ions from the 5d to the 4f state shows up as a luminescence band centred at a wavelength of ~550 nm (2.3 eV), which can be detected even at room temperature. To study the optical properties of Yb^{2+} in an $Al_2O_3:Yb_2O_3:SiO_2$ host, we used preform D, produced in a reducing atmosphere. Its UV transmission spectrum is presented in Fig. 4. Fitting the spectrum with Gaussians, we identified five absorption bands: at 3.1, 3.7, 4.1, 4.6 and 5.2 eV. According to Henke et al. [36], the bands at 3.1, 3.7 and 4.1 eV are attributable to Yb^{2+}.

The absorption bands of Yb^{2+} would be expected to show up as well in the spectrum of preform B after IR irradiation at a wavelength of 915 nm. Unfortunately, the shape of the spectrum of the irradiated sample (Fig. 5) was too complex to identify with certainty the known absorption bands of Yb^{2+}. Assuming that the absorption by Yb^{2+} was heavily obscured

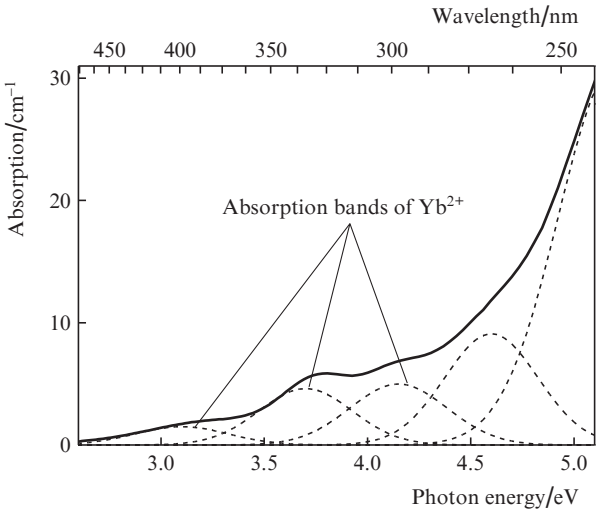

Figure 4. Initial UV absorption spectrum of sample D, containing Yb^{2+} ions.

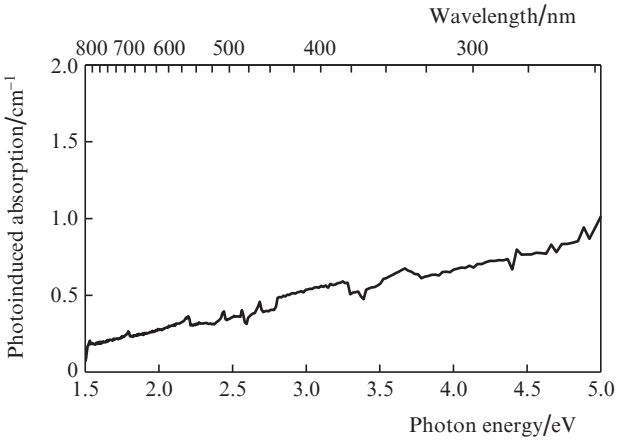

Figure 5. Photoinduced absorption spectrum of sample B after IR irradiation at a wavelength of 915 nm (1.3 eV).

by the stronger absorption in Al-OHCs, we attempted to find a way of eliminating or, at least, reducing its contribution. As follows from analysis of ESR spectra [38], Al-OHCs do not form when the glass network contains molecular hydrogen, which actively reacts with Al-OHCs to form stable hydroxyls, having no UV or visible absorption bands. In the presence of hydrogen, the photochemical reaction scheme takes the form

$$Yb^{3+}-O-Al + H \overset{h\nu}{\longleftrightarrow} Yb^{2+} + H-O-Al. \qquad (2)$$

Of special note is that this reaction is much less reversible than that represented by scheme (1) because of the high O–H bond energy. Thus, under given UV or IR irradiation conditions, Yb^{2+} ions will be generated in the glass network more efficiently in the presence of hydrogen than without it. The spectrum of sample B after H_2 loading followed by irradiation at a wavelength of 915 nm (Fig. 6) shows well-defined absorption bands of the Yb^{2+} ion at 3.1, 3.7 and 4.1 eV, the same as in the spectrum of sample D.

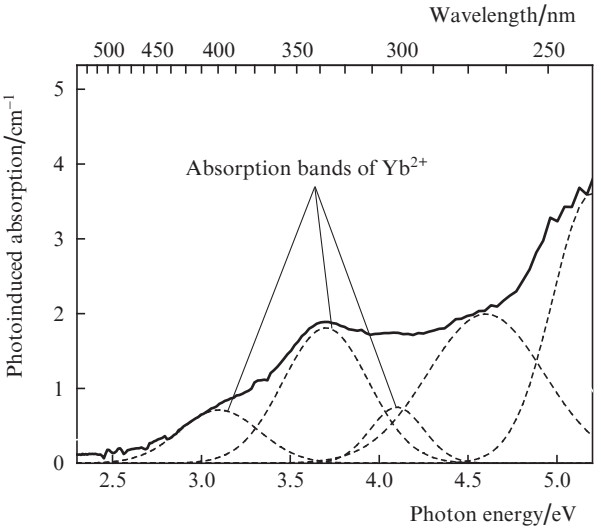

Figure 6. Photoinduced absorption spectrum of sample B after loading with molecular hydrogen followed by IR irradiation at a wavelength of 915 nm (1.3 eV).

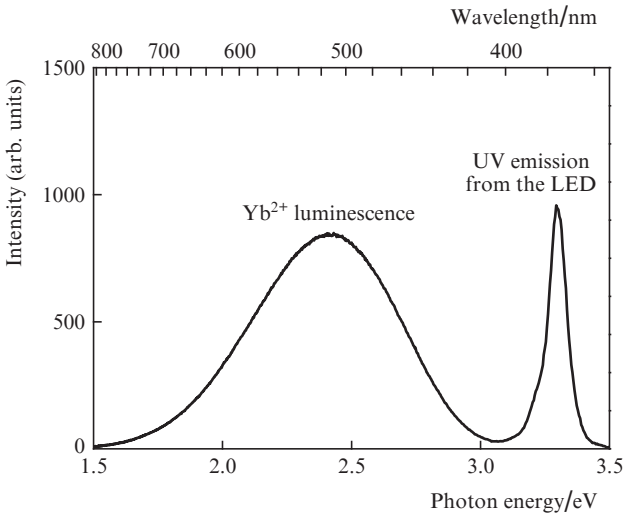

Figure 8. Luminescence spectrum of sample *D* under excitation with a UV LED at a wavelength of 380 nm (3.25 eV).

The presence of Yb^{2+} ions in samples B after UV and IR irradiation was also evidenced by the characteristic luminescence band centred near 2.3–2.4 eV. The luminescence was excited by a UV light emitting diode (LED) with a peak emission wavelength of 380 nm (3.25 eV), which is well within the absorption range of the Yb^{2+} ion. The LED beam was launched along the preform core axis, and the luminescence was detected at 90° to the input direction using a receiving fibre. It is seen in Fig. 7 that the luminescence spectra of the irradiated samples B are similar in shape to that of sample D (Fig. 8), with the highest luminescence intensity observed after H_2 loading. Note also that the scatter in the peak emission intensity of the UV LED in the luminescence spectra is due to variations in the photoinduced refractive index change in the core of the irradiated samples and should thus be left out of consideration.

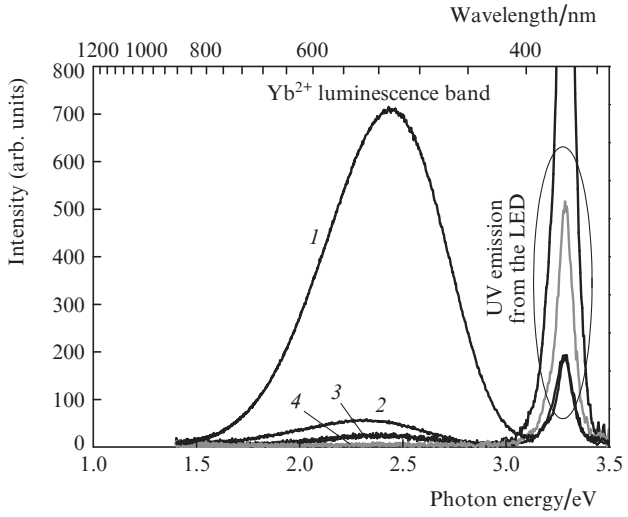

Figure 7. Luminescence spectra of samples B under excitation with a UV LED at a wavelength of 380 nm (3.25 eV): after H_2 loading followed by irradiation at λ = 193 nm (*1*), after irradiation at λ = 193 (*2*) and 915 nm (*3*) and without irradiation (*4*).

Thus, the absorption and luminescence bands of Yb^{2+} observed in the spectra of the irradiated $Al_2O_3:Yb_2O_3:SiO_2$ glass preforms provide conclusive evidence of $Yb^{3+} \rightarrow Yb^{2+}$ ion conversion in the photodarkening process in active fibres.

7. Discussion

Summarising the results on the absorption and luminescence spectra of sample B, we assign the absorption bands at 5.1 and 6.5 eV to Yb^{3+} transitions to a CTS. This hypothesis is supported by the fact that, under irradiation at 6.4 eV (which we believe to cause direct CTS excitation through UV photon absorption), the spectrum of sample B showed two emission bands at 2.3 and 3.5 eV, characteristic of CTL in aluminate crystals. Also, under UV irradiation we observed Yb^{3+} IR luminescence corresponding to the $^2F_{5/2} \rightarrow {}^2F_{7/2}$ transition, and the irradiated samples showed visible luminescence due to the Yb^{2+} ions that had resulted from the transition of some of the Yb^{3+} ions according to the scheme in Fig. 3.

Moreover, we believe that the scheme of the Yb^{3+} transition to Yb^{2+} in Fig. 3 is also valid in the case of cooperative CTS excitation under IR irradiation, which occurs when an Yb^{3+} ion absorbs the energy of several (at least four) neighbouring ions, equivalent to a UV photon energy (5–6 eV). In particular, after IR irradiation at an energy of 1.3 eV sample B showed Yb^{2+} luminescence, which indicates that the oxidation state of some of the ytterbium ions that experienced cooperative excitation to the CTS changed from +3 to +2. Thus, the $Yb^{3+} \rightarrow Yb^{2+}$ transition in $Al_2O_3:Yb_2O_3:SiO_2$ glass is similar to a model proposed previously for Yb:YAG and Yb:AG aluminate crystals [27] and, hence, occurs in the same way in the case of both cooperative and direct CTS excitation.

The present results lead us to conclude that the mechanism of photodarkening in active fibres under IR pumping at wavelengths in the range 915–976 nm includes initial cooperative CTS excitation of Yb^{3+} ions, which leads to electron capture at the ions from nearest neighbour oxygen

orbitals, and a final relaxation of the excited state of the entire complex in the form of a stable defect pair: reduced Yb^{2+} ion + Al-OHC hole centre. We believe that the contribution of the absorption band of Al-OHCs centred at 2.3 eV (540 nm) has a crucial effect on the growth of the optical loss in the visible and near-IR spectral regions (400–1000 nm).

It is also worth noting the marked shift (~1.5 eV) of the CT absorption peak of the $Al_2O_3:Yb_2O_3:SiO_2$ glass to longer wavelengths in comparison with $P_2O_5:Yb_2O_3:SiO_2$ glass studied previously [39], which has a peak at an energy of ~6.5 eV. The shift is one of the key factors that account for the low rate and saturation limit of photodarkening in $P_2O_5:Yb_2O_3:SiO_2$ fibres, first, because CTS excitation in such fibres requires interaction between not four but at least five closely spaced Yb^{3+} ions, which is a much less likely process and shows up as considerably slower photoinduced optical loss dynamics. Second, the increase in the smallest number of closely spaced Yb^{3+} ions necessary for cooperative interaction from four in $Al_2O_3:Yb_2O_3:SiO_2$ to five in $P_2O_5:Yb_2O_3:SiO_2$ sharply reduces the number of ytterbium clusters in the glass network in which CTS excitation is possible (it is this factor that we believe to be responsible for the low loss saturation level in $P_2O_5:Yb_2O_3:SiO_2$ fibres).

8. Conclusions

We have compared the luminescence spectra of $Al_2O_3:Yb_2O_3:SiO_2$ preforms and Yb:YAG crystals measured under UV irradiation at a wavelength of 193 nm (6.4 eV). The luminescence spectra of the preforms and crystals have been shown to contain bands corresponding to Yb^{3+} radiative relaxation from a charge transfer state. The bands at 5.1 and 6.5 eV in the initial UV absorption spectra of the $Al_2O_3:Yb_2O_3:SiO_2$ preforms correspond to Yb^{3+} transitions to the CTS. UV irradiation of the $Al_2O_3:Yb_2O_3:SiO_2$ core glass leads to photoinduced Yb^{3+} excitation to the CTS, a process similar to that reported previously for Yb:YAG crystals. The absorption spectra of the preforms after IR irradiation (915 nm) contain absorption bands of the Yb^{2+} ion, and the luminescence spectra of these samples contain a band centred at 2.3 eV (540 nm), corresponding to Yb^{2+} $5d \rightarrow 4f$ transitions.

Thus, the first experimental evidence has been provided that the photodarkening in $Al_2O_3:Yb_2O_3:SiO_2$ core glass is due to simultaneous generation of defect pairs each composed of an aluminium–oxygen hole centre and Yb^{2+} ion through photoinduced CTS excitation in Yb^{3+} ions, followed by electron capture at the ytterbium ion from one of the nearest neighbour oxygens.

Acknowledgements. This work was supported by the Russian Science Foundation (Grant No. 14-19-01572).

References

1. Koponen J., Söderlund M.J., Tammela S.K.T., Po H. *Proc. SPIE Int. Soc. Opt. Eng*., **5990**, 599008 (2005).
2. Shubin A., Yashkov M., Melkumov M., Smirnov S., Bufetov I., Dianov E. *CLEO/Europe-IQEC 2007* (Germany, Munich, 2007) CJ3-1-THU.
3. Manek-Hönninger I., Boullet J., Cardinal T., Guillen F., Ermeneux S., Podgorski M., Bello Doua R., Salin F. *Opt. Express*, **15** (4), 1606 (2007).
4. Arai T., Ichii K., Tanigawa S., Fujimakia M. *Proc. SPIE Int. Soc. Opt. Eng*., **7914**, 79140K (2011).
5. Rybaltovsky A.A., Aleshkina S.S., Likhachev M.E., Bubnov M.M., Umnikov A.A., Yashkov M.V., Gur'yanov A.N., Dianov E.M. *Kvantovaya Elektron*., **41** (12), 1073 (2011) [*Quantum Electron*., **41** (12), 1073 (2011)].
6. Sim F., Catlow C.R.A., Dupuis M., Watts J.D. *J. Chem. Phys.*, **95** (6), 4215 (1991).
7. Zyubin A.S., Mebel A.M., Lin S.H. *J. Chem. Phys.*, **119** (21), 11408 (2003).
8. Jetschke S., Unger S., Röpke U., Kirchhof J. *Opt. Express*, **15** (22), 14838 (2007).
9. Koponen J., Söderlund M.J., Hoffman H.J., Kliner D.A.V., Koplow J.P., Hotoleanu M. *Appl. Opt*., **47** (9), 1247 (2008).
10. Sen S., Rakhmatullin R., Gubaydullin R., Silakov A. *J. Non-Cryst. Solids*, **333**, 22 (2004).
11. Sen S., Rakhmatullin R., Gubaydullin R., Pöppl A. *Phys. Rev. B*, **74**, 100201 (2006).
12. Yoo S., Basu C., Boyland A.J., Sones C., Nilsson J., Sahu J.K., Payne D. *Opt. Lett*., **32** (12), 1626 (2007).
13. Carlson C.G., Keister K.E., Dragic P.D., Croteau A., Eden J.G. *J. Opt. Soc. Am. B*, **27** (10), 2087 (2010).
14. Mattsson K.E. *Opt. Express*, **19** (21), 19797 (2011).
15. Trukhin A.N., Troks J., Griscom D.L. *J. Non-Cryst. Solids*, **353**, 1560 (2007).
16. Griscom D.L. *J. Non-Cryst. Solids*, **357**, 1945 (2011).
17. Dragic P.D., Carlson C.G., Croteau A. *Opt. Express*, **16** (7), 4688 (2008).
18. Peretti R., Gonnet C., Jurdyc A.-M. *Proc. SPIE Int. Soc. Opt. Eng.*, **8257**, 825705 (2012).
19. Kirchhof J., Unger S., Jetschke S., Schwuchow A., Leich M., Reichel V. *Proc. SPIE Int. Soc. Opt. Eng*., **7195**, 71950S (2009).
20. Skuja L. *J. Non-Cryst. Solids*, **239**, 16 (1998).
21. Trukhin A., Poumellec B., Garapon J. *J. Non-Cryst. Solids*, **332**, 153 (2003).
22. Engholm M., Norin L. *Proc. SPIE Int. Soc. Opt. Eng.*, **7195**, 71950T (2009).
23. Rydberg S., Engholm M. *Opt. Express*, **21** (6), 6681 (2013).
24. Dianov E.M., Gerasimova E.I., Zavorotnyi Yu.S., Rybaltovskii A.O., Chernov P.V. *Fiz. Khim. Stekla*, **25** (2), 189 (1999).
25. Gerasimova E.I., Chernov P.V. *Fiz. Khim. Stekla*, **26** (4), 515 (2000).
26. Pieterson L., Heeroma M., Heer E., Meijerink A. *J. Lumin.*, **91**, 177 (2000).
27. Guerassimova N., Garnier N., Dujardin C., Petrosyan A.G., Pedrini C. *J. Lumin.*, **94–95**, 11 (2001).
28. Deschamps T., Ollier N., Vezin H., Gonnet C. *J. Chem. Phys.*, **136**, 014503 (2012).
29. Kir'yanov A.V., Barmenkov Yu.O., Mendoza-Santoyo F., Cruz J.L., Andres M.V. *Laser Phys. Lett*., **12** (5), 898 (2008).
30. Ollier N., Doualan J.-L., Pukhkaya V., Charpentier T., Moncorgé R., Sen S. *J. Non-Cryst. Solids*, **357**, 1037 (2011).
31. Xu Y.-N., Ching W.Y. *Phys. Rev. B*, **59** (16), 10530 (1999).
32. Chen Y.F., Lim P.K., Lim S.J., Yang Y.J., Hu L.J., Chiang H.P., Tse W.S. *J. Raman Spectrosc.*, **34**, 882 (2003).
33. Sampaio J.A., Gama S. *Phys. Rev. B*, **69**, 104203 (2004).
34. Krasikov D.N., Scherbinin A.V., Vasil'ev A.N., Kamenskikh I.A., Mikhailin V.V. *J. Lumin.*, **128**, 1748 (2008).
35. Ishi T. *J. Chem. Phys.*, **122**, 024705 (2005).
36. Henke M., Perßon J., Kück S. *J. Lumin.*, **87–89**, 1049 (2000).

37. Kirchhof J., Unger S., Schwuchow A., Jetschke S., Reichel V., Leich M., Scheffel A. *Proc. SPIE Int. Soc. Opt. Eng.*, **7598**, 75980B (2010).
38. Hentz R.R., Wickenden D.K. *J. Phys. Chem.*, **73** (4), 817 (1969).
39. Rybaltovsky A.A., Umnikov A.A., Bobkov K.K., Lipatov D.S., Romanov A.N., Likhachev M.E., Sulimov V.B., Gur'yanov A.N., Bubnov M.M., Dianov E.M. *Kvantovaya Elektron.*, **43** (11), 1037 (2013) [*Quantum Electron.*, **43** (11), 1037 (2013)].